nature energy

Article

https://doi.org/10.1038/s41560-023-01304-w

Climate change impacts on planned supply–demand match in global wind and solar energy systems

Received: 4 August 2022

Accepted: 13 June 2023

Published online: 24 July 2023

Check for updates

Laibao Liu[1,2,3] ✉, Gang He[4,5], Mengxi Wu[6,7] ✉, Gang Liu[1], Haoran Zhang[8], Ying Chen[9], Jiashu Shen[1,2] & Shuangcheng Li[1,2]

Climate change modulates both energy demand and wind and solar energy supply but a globally synthetic analysis of supply–demand match (SDM) is lacking. Here, we use 12 state-of-the-art climate models to assess climate change impacts on SDM, quantified by the fraction of demand met by local wind or solar supply. For energy systems with varying dependence on wind or solar supply, up to 32% or 44% of non-Antarctic land areas, respectively, are projected to experience robust SDM reductions by the end of this century under an intermediate emission scenario. Smaller and more variable supply reduces SDM at northern middle-to-high latitudes, whereas reduced heating demand alleviates or reverses SDM reductions remarkably. By contrast, despite supply increases at low latitudes, raised cooling demand reduces SDM substantially. Changes in climate extremes and climate mean make size-comparable contributions. Our results provide early warnings for energy sectors in climate change adaptation.

With growing numbers of countries committed to achieving net-zero emissions energy system transitions, low-carbon and renewable wind and solar energy are undergoing unprecedented growth[1,2]. Continuing fast-falling costs of wind and solar power generations further accelerate this green energy revolution[3]. The International Energy Agency (IEA) projects that wind and solar energy might contribute to ~62% of the world's electricity generation and ~26% of its total energy supply by 2050 in the Sustainable Development Scenario[1].

Growing evidence shows that the vital role of wind and solar in the transition pathways is complicated by climate change[4–7]. Both supply and demand sides of wind and solar energy systems are vulnerable to climate change, raising concerns about their anticipated efficacy under climate change[8]. On the supply side, weather-dependent wind and solar power generation is directly controlled by changes in meteorological inputs, mainly temperature, wind speed and solar irradiance[9–12]. For instance, climate change is likely to shift the geophysical pattern and size of wind; more frequent extreme wind events can shut down the wind turbine and thus block power outputs more often. On the demand side, a warming climate generally requires less demand for heating but more demand for cooling[5,13]. More temperature-related weather extremes, such as heatwaves and cold extremes, can also provoke sudden demand surges[14].

However, compared to investigating supply and demand separately, combining climate change impacts on supply and demand together is more critical for the safe and steady operation of energy systems because they need supply to match demand instantly. Furthermore, climate

[1]College of Urban and Environmental Sciences, Peking University, Beijing, China. [2]Key Laboratory for Earth Surface Processes of the Ministry of Education, Peking University, Beijing, China. [3]Institute for Atmospheric and Climate Science, ETH Zurich, Zurich, Switzerland. [4]Department of Technology and Society, College of Engineering and Applied Sciences, Stony Brook University, Stony Brook, NY, USA. [5]Marxe School of Public and International Affairs, Baruch College, City University of New York, New York, NY, USA. [6]Joint Institute for Regional Earth System Science and Engineering (JIFRESSE), University of California Los Angeles, Los Angeles, CA, USA. [7]Department of Earth, Environmental and Planetary Sciences, Brown University, Providence, RI, USA. [8]The Bartlett School of Sustainable Construction, University College London, London, UK. [9]School of Geography, Earth and Environmental Sciences, University of Birmingham, Birmingham, UK. ✉e-mail: liulb15@pku.edu.cn; mwu16@g.ucla.edu

https://doi.org/10.1038/s41560-023-01304-w

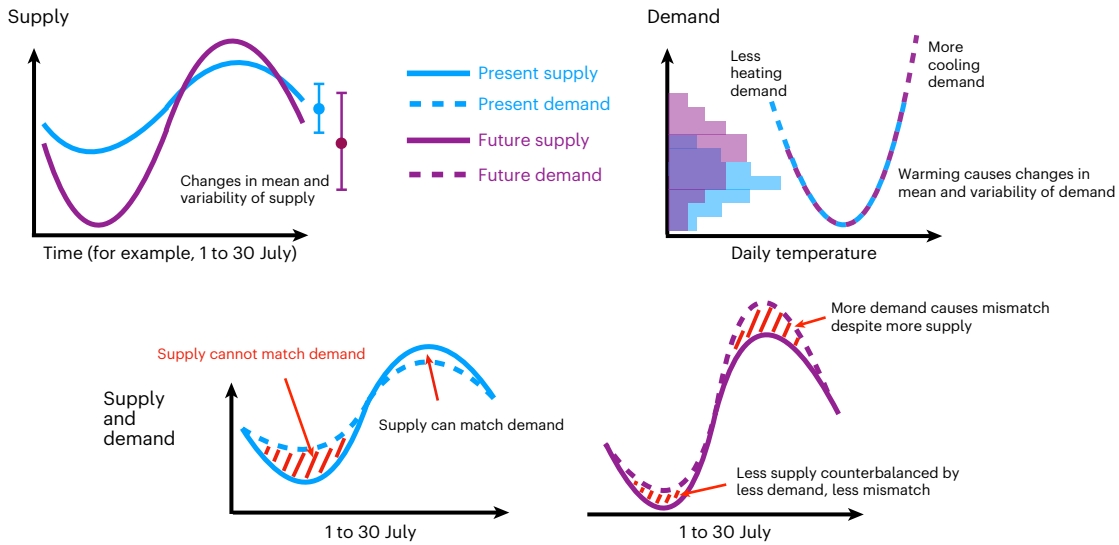

Fig. 1 | Conceptual illustrations of climate change impacts on supply, demand and SDM of wind and solar energy systems. In the supply graph, the error bars show the mean (dots) and 1 s.d. (vertical lines) of daily supply during a specific period. In the demand graph, the histograms show the distribution of daily energy demand during a specific period. In the supply and demand graph, the red slashing areas show the supply–demand mismatch (SDMM). With climate change, changes in climate impact-drivers (wind speed, temperature and radiation) could force wind or solar supply to increase or be more variable at some time; fewer cold weather conditions induce less heating demand while more hot weather conditions cause more cooling demands. Consequently, the SDMM would require additional power sources for generating supply to meet demand; otherwise the SDMM would cause power outages.

change impact investigations tend to look at changes of climate mean (long-term mean of climate state) while the impacts of climate variability (for example, extreme weather events) remain largely unknown. In addition, there are still knowledge gaps in some regions that are vital for global wind and solar energy developments, such as Central Asia and China[8]. Quantifying these impacts is imperative because if the supply–demand match (SDM) gets deteriorated by climate change, it might cause more power outages, leaving severe cascading consequences on society and the economy[15]. However, a systematic and consistent multimodel assessment of climate change impacts on SDM for wind and solar systems is still lacking at the global scale.

Here, we systematically assess the impact of climate change on SDM of energy systems planning low-to-high dependence levels on local wind or solar energy supply under various climate change scenarios based on 12 state-of-the-art global climate models (GCMs) participating in the Coupled Model Intercomparison Project Phase 6 (CMIP6). Our results show that climate change is likely to undermine the planned SDM in a relative sense in many regions of the world. Changes in supply and demand caused by climate change could be in opposite signs at a specific location, offsetting the negative synthetic effects of SDM to some extent. The importance of changes in climate variability is comparable to climate mean changes. We suggest that energy planners in regions where climate change undermines SDM need to adapt to climate change impacts on wind and solar energy systems.

Approach

Figure1 provides the conceptual illustration of climate change impacts on supply, demand and their consequences on the SDM. We first create the SDM index as the fraction of total demand met by local wind or solar supply over a temporal period:

$$D_{\mathrm{met},t} = \begin{cases} D_t, S_t \geq D_t \\ S_t, S_t < D_t \end{cases}, t \in [1, n]$$
$$\mathrm{SDM} = \frac{\sum_1^n D_{\mathrm{met},t}}{\sum_1^n D_t} \times 100\% \quad (1)$$

where t is time step (day) spanning from first to nth (GCMs provide daily simulations of variables for wind and solar energy assessments); D is demand; S is wind or solar supply; D_{met} is demand met by supply; S of 0 indicates no supply available to meet demand; SDM of 100% means a full match; and SDM of 0% means a least match. To be specific, for each grid cell, we assume that there is a planned local energy system with dependence on wind or solar supply. The local energy system may be a few households, a county or a city. The planned level of dependence can be achieved under present climate, denoted by $\mathrm{SDM}_{\mathrm{present}}$, and is assumed to be 25%, 50% and 75% for low, medium and high levels of dependence scenarios, respectively. $\mathrm{SDM}_{\mathrm{present}}$ indicates the fraction of total demand met by the local wind or solar supply over a period representing the present climate (1985–2014). Each energy planner or stakeholder within a given grid cell can make general estimates of the unmet demand by combining their demand and SDM. Daily variations of heating and cooling demand are computed according to temperature: hot days lead to higher demand for cooling and cold days lead to higher demand for heating. To achieve each planned $\mathrm{SDM}_{\mathrm{present}}$, the required installation area (IA) can be derived according to the demand and wind/solar power density. Daily variations of supply are then computed on the basis of the wind/solar power density and the IA (Methods).

To isolate climate change impacts, only climate impact-drivers (wind speed, temperature and radiation) are allowed to modulate SDM; non-climatic conditions (for example, IA) are kept constant. Therefore, relative changes of supply, demand and SDM are only caused by climate change. Long-term climate change impacts on SDM are quantified by the differences between estimated SDM based on future climate (2071–2100) and present climate (1985–2014): $\Delta\mathrm{SDM} = (\mathrm{SDM}_{2071\text{–}2100} - \mathrm{SDM}_{1985\text{–}2014})/\mathrm{SDM}_{1985\text{–}2014} \times 100\%$, in which t in equation (1) spans from the first day of the first year to the final day of the 30th year. Mid-term (2041–2070) climate change impacts on SDM are also assessed: $\Delta\mathrm{SDM} = (\mathrm{SDM}_{2041\text{–}2070} - \mathrm{SDM}_{1985\text{–}2014})/\mathrm{SDM}_{1985\text{–}2014} \times 100\%$. Future climate projections are from two shared socioeconomic pathway scenarios (SSP 245 and SSP 585). SSP 245 is an intermediate emission scenario while SSP 585 is a very high-emission scenario. First, we assess climate change impacts on the supply and demand separately and disentangle their respective consequences on SDM. In addition, we perform

https://doi.org/10.1038/s41560-023-01304-w

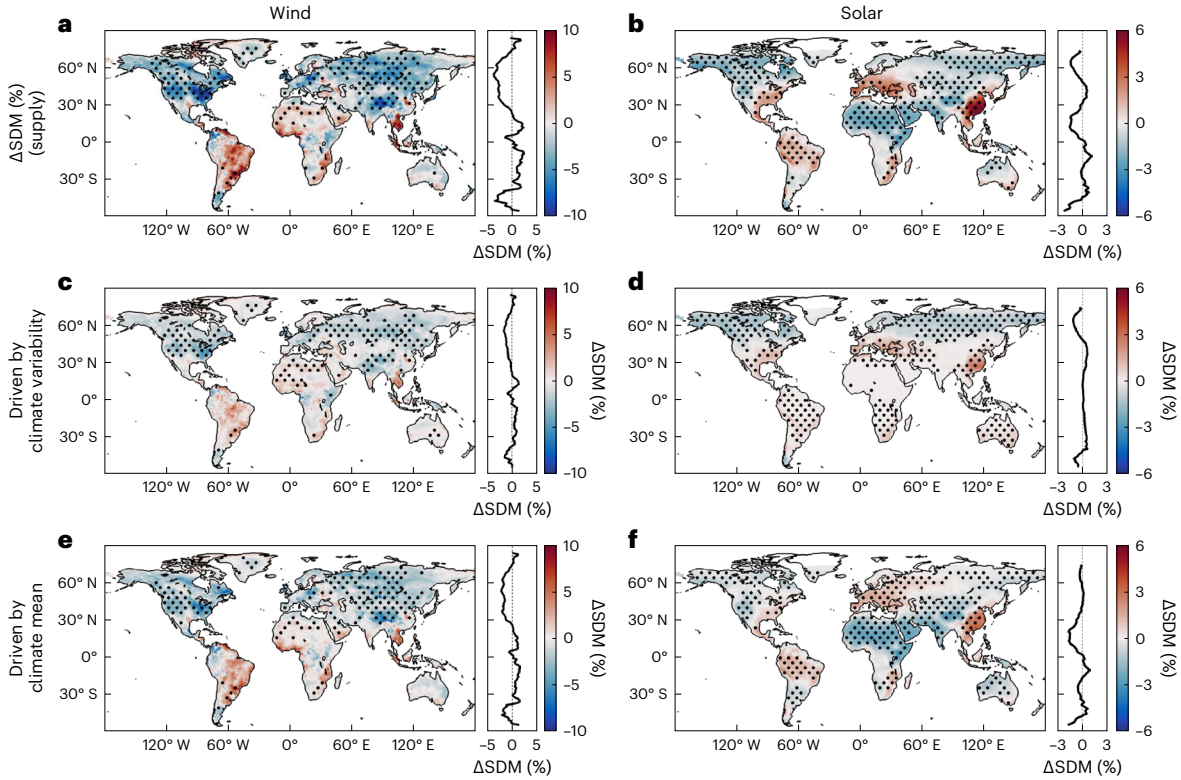

Fig. 2 | Climate change impacts on SDM arising from supply alone for wind and solar systems globally. a,**b**, Changes in SDM from 1985–2015 to 2071–2100 based on multimodel-mean estimates for energy systems with high dependence on wind (**a**) and solar (**b**) supply under SSP 245. The right panels show the profile of zonally integrated SDM changes (%). **c**–**f**, Corresponding contributions of climate variability (**c**,**d**) and climate mean (**e**,**f**) to SDM changes for wind (**c**,**e**) and solar energy (**d**,**f**) systems. Stippling indicates regions where the detected changes are considered to be robust; that is, 9 out of 12 models in the cluster agree on the sign of the changes. Latitude is shown on *y* axes; longitude is on *x* axes. Solid black lines show the profile of zonally integrated SDM changes.

control experiments to disentangle relative contributions of climate mean-induced supply/demand mean and climate variability-induced supply/demand variability to SDM changes. Then, we combine changes of supply and demand together and explore whether combining them would 'counterbalance' or 'enlarge' SDM changes driven by supply/demand alone (Methods).

Supply-driven SDM changes with controlled demand

Controlling demand is invariant to temperature changes, supply alone is projected to force about 25% and 37% of land areas (excluding Antarctica) to experience robust reductions of SDM for energy systems with a high dependence on wind and solar energy supply (referred to as wind and solar energy system hereafter) under SSP 245, respectively (Fig. 2a,b). For wind systems, SDM reductions are widespread across northern middle-to-high latitudes (NMH) (>30° N), pronounced in western North America (−4%), eastern North America (−6%), western and central Europe (−2%) and Eastern Siberia (−4%). Intensified variability and smaller mean of supply can explain 40% and 60% of SDM reductions, respectively (Fig. 2c,e and Supplementary Fig. 1). SDM increases are projected in many regions at low latitudes on average (30° S–30° N) but with larger uncertainty, such as northern South America (+2%), western Africa (+3%) and Sahara (+1%). These SDM increases are caused by larger mean and less variability of wind energy supply, consistent with a recent global assessment on wind power resources based on ten previous versions of climate models[16].

Like wind energy systems, SDM reductions of solar energy systems are also widespread across NMH. Compared to wind, solar systems are projected to experience smaller SDM reductions in magnitude globally and might also slightly gain SDM at some low-latitude regions, such as eastern Asia (+3%), northern South America (+1%) and the Mediterranean (+1%). At NMH, intensified variability and smaller mean explain 51% and 49% of SDM reductions, respectively (Fig. 2d,f). At low latitudes, benefits from weakened supply variability on SDM are counterbalanced by smaller supply mean across many regions, and supply variability and mean explain 18% and 82% of SDM changes, respectively. Additionally, projected relative changes of SDM in energy systems with lower dependence levels on wind and solar energy show similar spatial patterns but are greater in magnitude (for example, 2 and 1.3 times on average in the middle-dependence scenario, respectively); compared to SSP 245, projected relative SDM changes under SSP 585 show similar spatial patterns but are about 1.4 and 2.7 times in magnitude on average for wind and solar energy systems, respectively (Supplementary Fig. 2).

Demand-driven SDM changes with controlled supply

The actual sensitivity of heating and cooling demands to warming per degree is highly variable, depending on the local energy infrastructure, social-economic level, user behaviour and so on[8,17]. Therefore, according to previous efforts[5,18–23], we design two scenarios to include the likely range of demand responses to warming for each location: (1) a high-sensitivity one: the sensitivity of demand changes to heating and cooling (β_{heat} and β_{cool}) is 5% per °C and 8% per °C, respectively; and (2) a low-sensitivity one: β_{heat} and β_{cool} are 2% per °C and 3% per °C, respectively. To disentangle the effects of demand on SDM changes alone, present and future supply–demand profiles only differ in the demand (Methods). In the high-sensitive scenario and SSP 245, demand-induced SDM changes are more spatially uniform than that caused by supply alone and show apparently opposite signs on two sides of around 30° N (Fig. 3a,b). This apparent spatial pattern is consistent with the recent

https://doi.org/10.1038/s41560-023-01304-w

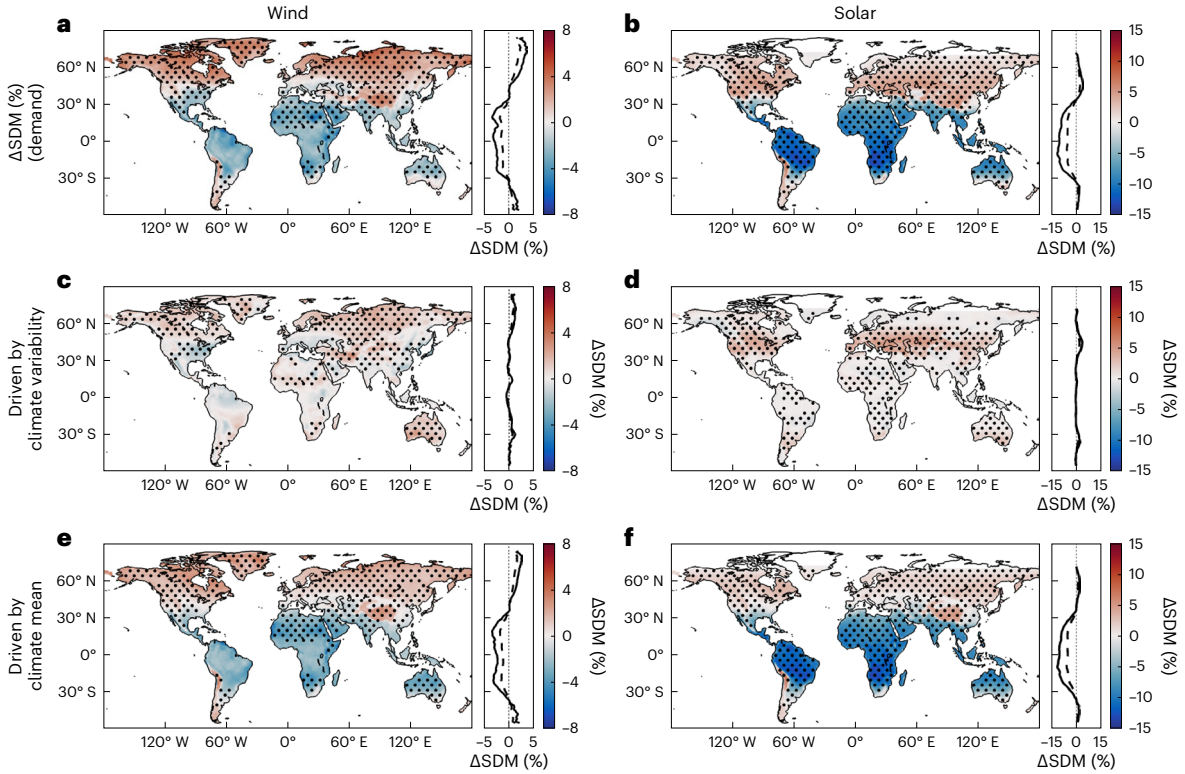

Fig. 3 | Climate change impacts on SDM arising from demand alone for wind and solar systems globally. a,**b**, Changes in SDM from 1985–2015 to 2071–2100 based on multimodel-mean estimates for energy systems with high dependence on wind (**a**) and solar supply (**b**) under SSP 245. The right panels show the profile of zonally integrated SDM changes in the high-sensitivity demand scenario (solid line) and the low-sensitivity demand scenario (dashed line) (%). **c**–**f**, Corresponding contributions of climate variability (**c**,**d**) and climate mean (**e**,**f**) to SDM changes for wind (**c**,**e**) and solar energy (**d**,**f**) systems. Stippling indicates regions where the detected changes are considered to be robust; that is, 9 out of 12 models in the cluster agree on the sign of the changes. Latitude is shown on *y* axes; longitude is on *x* axes.

assessment of climate change impacts on global electricity consumption[5,21]. Specifically, SDM increases about 1% and 2% at NMH but decreases −2% and −8% at south of 30° N for wind and solar systems, respectively. This underlines the dependence of the degree of trade-offs between rising cooling demands and declining heating demands on background climate, mainly determined by the latitude. At NMH, less required heating demands with a warming climate counterbalance raised cooling demands, contributing 60% and 55% to SDM increases for wind and solar systems, respectively (Fig. 3e,f and Supplementary Fig. 3) and weakened demand variability also contributes 45% to SDM increases for solar systems (Fig. 3d). By contrast, at low latitudes, more required cooling demands largely increase total demands in mean, explaining 84% and 95% of SDM reductions for wind and solar systems, respectively. Additionally, compared to the high-dependence scenario, relative changes of SDM in energy systems with lower dependence levels on wind and solar energy are amplified in magnitude (for example, 2.2 and 1.7 times on average in middle-dependence scenario, respectively); compared to SSP 245, SDM changes under SSP 585 are about 1.8 and 2.2 times in magnitude on average for wind and solar systems, respectively (Supplementary Fig. 4).

SDM changes driven by both supply and demand

Taking climate change impacts on both supply and demand into account, the resulting SDM changes show different patterns compared to that driven by supply or demand alone. At NMH, unlike supply-induced universal SDM reductions, it is apparent that smaller mean and less variability of demand can alleviate negative impacts from supply remarkably (Fig. 4a,b): this is most pronounced for solar systems, with SDM shifting from losses to gains there (−0.4% to +4%); wind systems experience less SDM losses (−3% to −2%) but would still suffer from large SDM reductions in eastern North America (−10%), western and central Europe (−2%) and so on. By contrast, at low latitudes, large rises in cooling demands would still cause widespread SDM reductions for wind and solar systems, despite the benefits in supply from climate change for some regions here. The land area fraction of low latitudes with robust SDM reductions (27% and 73%) is 5.4 and 2.2 times larger than that caused by the supply side alone for wind and solar energy systems, respectively. In total, 27% and 40% of land areas are projected to experience robust SDM reductions for wind and solar energy systems, respectively. Climate variability can also make size-comparable contributions to future SDM changes compared to climate mean (Supplementary Fig. 5). Additionally, for energy systems with lower dependence levels on local wind and solar energy supply, land areas projected to experience robust SDM reductions are a bit larger (for example, 32% and 44% of land areas for wind and solar systems in the low-dependence scenario, respectively); there are larger changes of SDM under SSP 585 than that under SSP 245 (higher by 10% and 16% for wind and solar systems on average) (Supplementary Fig. 6).

Daily frequency and intensity of supply–demand mismatch

Different from the previously assessed SDM at a 30-year timescale (t in equation (1) spans from first day of first year to final day of 30th year), we further investigate SDM at a daily scale (n in equation (1) is 1). By adopting the framework of investigating climate and weather extremes (for example, droughts and heatwaves) from climate science, we also define supply–demand mismatch (SDMM: 100% − SDM) and two metrics for easy understanding: (1) SDMM frequency—the proportion of days with daily SDM <100% and (2) SDMM intensity—the

https://doi.org/10.1038/s41560-023-01304-w

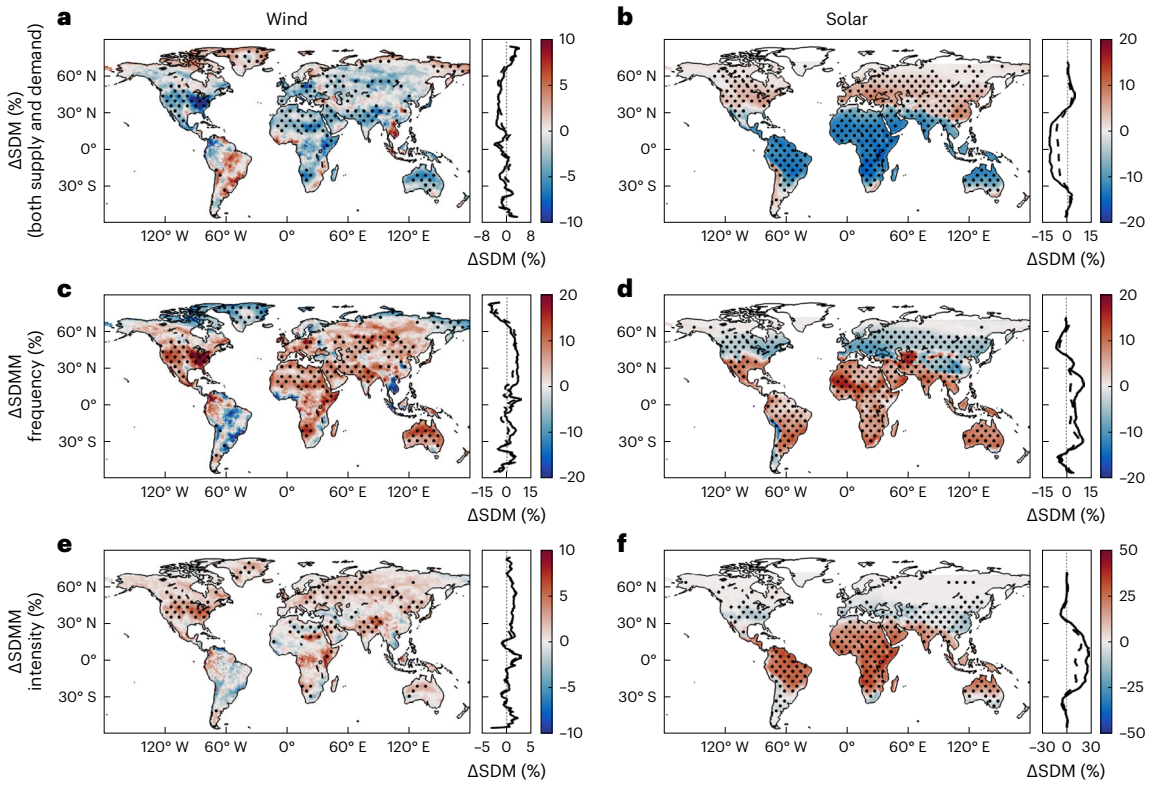

Fig. 4 | Climate change impacts on SDM arising from both supply and demand for wind and solar systems globally. a,**b**, Changes in SDM from 1985–2015 to 2071–2100 based on multimodel-mean estimates for energy systems with high dependence on wind (**a**) and solar supply (**b**) under SSP 245. The right panels show the profile of zonally integrated SDM changes in the high-sensitivity demand scenario (solid line) and low-sensitivity demand scenario (dashed line) (%). **c**–**f**, Corresponding changes in daily SDMM frequency and intensity for wind (**c**,**f**) and solar energy (**d**,**f**) systems. Stippling indicates regions where the detected changes are considered to be robust; that is, 9 out of 12 models in the cluster agree on the sign of the changes. Latitude is shown on *y* axes; longitude is on *x* axes.

average fraction of unmet demand to total demand during days with daily SDM <100%. The frequency and intensity of SDMM for wind and solar systems are projected to increase considerably globally under SSP 245 (Fig. 4c–f). As expected, increasing frequency and intensity of SDMM always co-occur with decreasing SDM. In regions with robust SDM reductions, the frequency of SDMM is projected to increase 9% and 7% for wind and solar systems, respectively; solar systems show a much larger increase of SDMM intensity (+19%) than do wind systems (+2%).

Additionally, to provide the available base of assessments for interested parties worldwide, we give regional sheets to elaborate regional average impacts of climate change on supply, demand and the resulting SDM for wind and solar energy systems (Fig. 5).

Climate change adaptation

More greenhouse gas emissions raise levels of climate change and consequent negative impacts on SDM, as shown in the high-emission scenario (Supplementary Figs. 7 and 8). Additionally, we propose two climate change adaptation strategies. In the first one, we add energy storage spanning from 1 to 20 days (in units of equivalent daily mean energy demand under present climate) to future energy systems. To prevent negative impacts of climate change on present SDM, energy systems with high dependence on wind energy supply require about 2 days of energy storage on average (Supplementary Fig. 9a), while adding energy storage up to 20 days is still insufficient for solar systems across most regions (stipples in Supplementary Fig. 9b). Also, adding energy storage cannot mitigate the increasing frequency and intensity of SDMM of solar systems but work well for the increasing SDMM frequency of wind systems (Supplementary Fig. 10a–d). In the second strategy, we increase the power generation IA in the future by the factor of 0.1 to 1. On average, 26% and 25% of increment are sufficient to prevent SDM reductions from climate change for wind and solar energy systems, respectively, except for parts of wind systems in eastern North America and Central Africa (Supplementary Fig. 9c,d). A larger IA to generate more energy supply can reduce the increases in SDMM frequency and intensity of wind and solar systems across most regions (Supplementary Fig. 10e–h).

Discussion and conclusions

Here, we provide a systematic and consistent multimodel assessment of climate change impacts on both supply and demand for wind and solar energy systems ranging from the grid-cell scale to global scales with 12 state-of-the-art GCMs. SDM index is created to capture the synthetic effects of supply and demand on energy systems from climate change.

Energy systems must match demand with supply simultaneously. We emphasize that investigating either supply or demand alone cannot offer an holistic understanding of the vulnerability of energy systems to climate change and could cause inevitable overestimations or underestimations. For instance, the increased energy supply at low latitudes under climate change[16] can be counterbalanced by raised cooling demands with a warming climate; projected decreased supply at northern middle-to-high latitudes[10,24] can be alleviated a lot by declined heating demands. Furthermore, it is critical to take future changes of climate variability into account, in addition to changes of climate mean. Climate and weather extremes are well investigated in the climate science community[25]; we integrate them into energy systems and demonstrate that they can make size-comparable contributions to SDM reductions compared with commonly assessed impacts of the climate mean changes[4]. Despite growing studies of climate change impacts on

https://doi.org/10.1038/s41560-023-01304-w

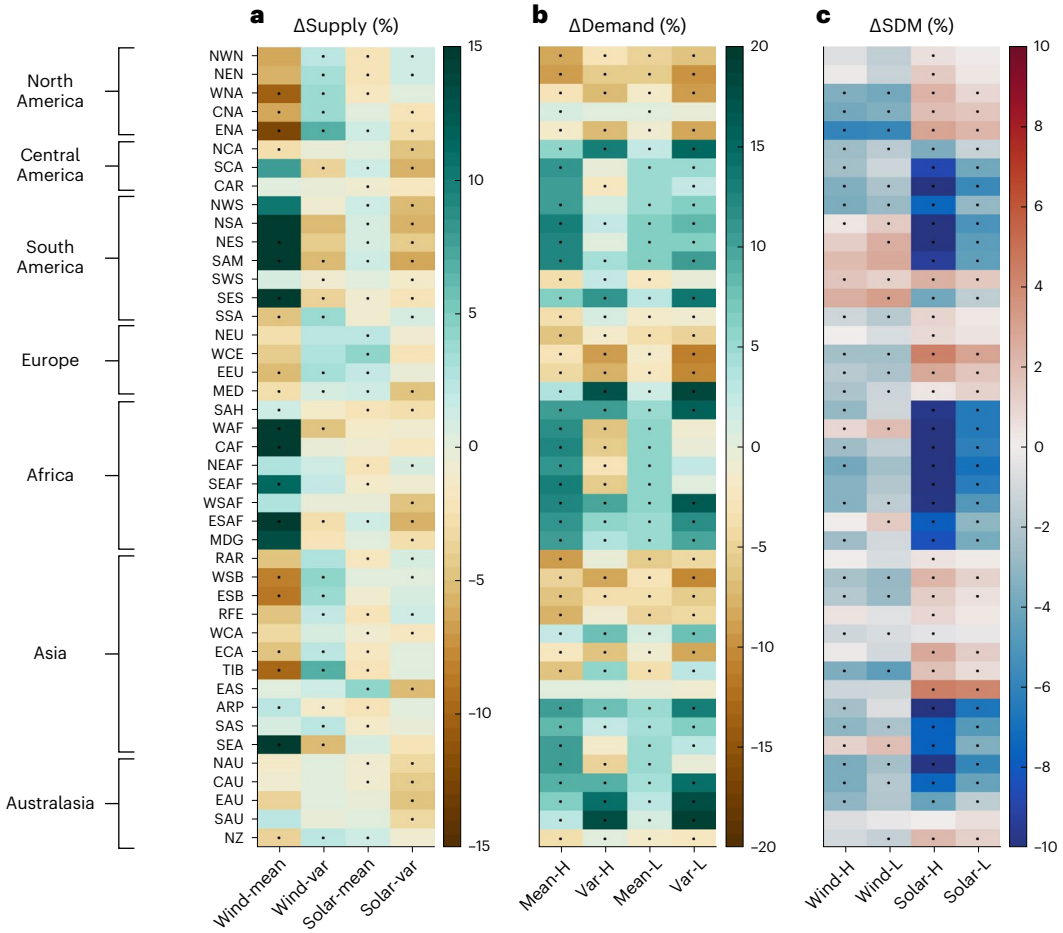

Fig. 5 | Regional climate change impacts on supply, demand and SDM for wind and solar systems globally. a,**b**, Changes in the mean and variability (coefficient of variation) of supply (**a**) and demand (**b**) from 1985–2015 to 2071–2100 based on multimodel-mean estimates under SSP 245. For demand, H and L indicate the high-sensitive and low-sensitive scenario, respectively. **c**, Changes in SDM from 1985–2015 to 2071–2100 for energy systems with high dependence on wind and solar supply under SSP 245. Stippling indicates regions where the detected changes are considered to be robust; that is, 9 out of 12 models in the cluster agree on the sign of the changes. The regional classification is adopted from the sixth IPCC Working Group I reference[43]. NWN, north western North America; NEN, north eastern North America; WNA, west North America; CNA, central North America; ENA, east North America; NCA, north Central America; SCA, south Central America; CAR, Caribbean; NWS, north western South America; NSA, north South America; NES, north eastern South America; SAM, South American monsoon; SWS, south western South America; SES, south eastern South America; SSA, south South America; NEU, north eastern Europe; WCE, west and central Europe; EEU, east Europe; MED, Mediterranean; SAH, Sahara; WAF, west Africa; CAF, central Africa; NEAF, north eastern Africa; SEAF, south eastern Africa; WSAF, west southern Africa; ESAF, east southern Africa; MDG, Madagascar; RAR, Russian Arctic; WSB, west Siberia; ESB, east Siberia; RFE, Russian Far East; WCA, west central Asia; ECA, east central Asia; TIB, Tibetan Plateau; EAS, east Asia; ARP, Arabian Peninsula; SAS, south Asia; SEA, south eastern Asia; NAU, north Australia; CAU, central Australia; EAU, east Australia; SAU, south Australia; NZ, New Zealand; Var, variability.

wind and solar energy systems in the past decade, there are still many regional gaps. For example, data and analysis of climate impacts on wind or/and solar energy in the Middle East, North Africa and South Asia, China and so on, are still missing[8]. Our global grid-cell assessment fills critical gaps about supply/demand and SDM in these understudied regions that are essential for global wind and solar developments.

Wind and solar energy system infrastructures are always fixed assets that last decades. Our results underline the necessity to prepare for climate change adaptations when planning. Global hotspot regions of negative climate change impact and corresponding adaptation needs of energy storage and IA are provided from the technical perspective. In reality, adding storage might not be economic for cases with great demand. Increasing IA is an effective strategy but is possibly limited by the realistic energy system infrastructure and policy constraints. For instance, for each household that plans photovoltaics (PV) on the roof, if all roof areas for PV panels are planned to be used under present climate, adding extra IA might be less practicable under climate change. Demand-side adaptation strategies, such as better home insulation[26], heating/cooling system efficiency improvement[27] and ventilation system implementation[28], can reduce the sensitivity of demand response to climate change and then alleviate climate-driven demand increase. If these strategies are well implemented, SDM reductions arising from the demand side are anticipated to be lowered to some extent. We state that the estimated climate change impacts on supply, demand and SDM in this study also precede any adaptation strategies[5]. Integrated Assessment models or Computable General Equilibrium models can take both our estimates and socioeconomic factors into account to derive ex post actual energy supply, demand and SDM. In addition, since climate change impacts on wind and solar energy systems can diverge at the same location (for example, wind SDM increase but solar SDM decrease in South America), the mix of wind and solar energy systems, if allowed, could be very useful. Besides, it is well documented that aggregating wind and solar power generation at a larger spatial scale can reduce the intermittency of power generation[29,30]; strengthening grid connections might be another option for climate change adaptation.

We acknowledge that energy system operation is more complicated than our analysis. For example, power transmissions are also vulnerable to climate change[31,32] and might change the spatial and temporal balance of supply and demand; the power system might also run at a spatial scale which does not overlap exactly with our grid cell[33]; technology improvements probably overcome some climate change impacts[34]. In addition, although we already used the latest CMIP6 GCMs, the accuracy of regional or local wind energy assessment can be further improved using climate simulations with finer spatial resolution, especially in regions with complex terrain[35]. Bias correction of wind speed with local wind mast observations is useful to reduce model uncertainties; for instance, more realistic parameters in power law extrapolation[36]. Therefore, careful integration of climate models with energy system models is highly recommended to inform comprehensive and accurate climate change impacts in specific regions[37–39]. Nevertheless, our study reveals how climate change could impact the supply-and-demand match globally. Such global assessments at a finer scale provide the foundation for future analyses integrating with realistic power systems.

Given the pivotal and rising role of wind and solar energy systems in mitigating climate change and achieving sustainable development, we demonstrate that climate change is likely to undermine the planned match between energy demand and wind and solar energy supply in a relative sense across many regions globally. The planned supply–demand match refers to the fraction of demand met by local wind or solar supply. We suggest that energy system plans prepare for possible negative impacts from changes in both climate mean and climate variability. This study provides early warnings for energy sectors in adapting to climate change impacts on wind and solar energy systems.

Methods

Global climate models

This study uses the daily outputs of climate simulations from 12 state-of-the-art GCMs participating in the CMIP6, including: ACCESS-ESM1-5, BCC-CSM2-MR, CanESM5, CESM2, CMCC-ESM2, GFDL-ESM4, IPSL-CM6A-LR, MPI-ESM1-2-HR, NorESM2-MM, UKESM1-0-LL, MRI-ESM2-0 and EC-Earth3 (Supplementary Table 1). The GCMs are selected from different providers/institutes to ensure a relatively fair distribution and representativeness. We use the output of downwelling shortwave irradiance (rsds), surface wind speed (sfcWind) and near-surface air temperature (tas) from GCMs as the input to compute global wind power and solar power density.

For the present climate, we use 30-yr simulations from the 'historical' scenario spanning from 1985 to 2014, which is driven by all historical forcings. For the future climate, we used 30-yr simulations from the SSP 245 scenario and SSP 585 scenario spanning from 2041 to 2100. SSP 245 is an intermediate emission scenario where the CO_2 emission remains close to the present level in the first half of the century and then starts to decrease due to strong mitigation. In this scenario, the atmospheric CO_2 concentration continues to increase but the increasing speed slows down approaching the end of the century. The projected global surface temperature increase by 2100 is probably between 2.1 °C and 3.5 °C, relative to 1850–1900. SSP 585 is a very high-emission scenario where human society is assumed to continue to rely on fossil fuels. This scenario may be less plausible with the transformation of the energy section. In this scenario, the CO_2 emission at the end of the century is about three to four times higher than the present and the atmospheric CO_2 concentration also grows above 1,000 ppm. The projected global surface temperature increase by 2100 is probably between 3.3 °C and 5.7 °C, relative to 1850–1900 (ref. 40).

Wind power density

Wind power production is mostly a function of the instantaneous wind speed (U). When the wind speed is higher than the cut-in speed, U_{min}, and lower than the speed required for the nameplate capacity (U_c), instantaneous wind power production (E_{wind}) is the product of air density (ρ), swept area of the blades (A) and the wind speed cubed (U^3):

$$E_{wind} = 1/2\rho A U^3 \tag{2}$$

Wind power production remains constant after reaching the nameplate capacity until the wind turbine is shut down when the wind speed is too strong (U_{max}). Following a recent review[9], the constants 4 m s^{-1}, 13.5 m s^{-1} and 25 m s^{-1} are assumed for U_{min}, U_c and U_{max}, respectively. Air density (ρ) at the surface is considered constant at 1.225 kg m^{-3}. Therefore, the full relationship between the instantaneous wind speed and the instantaneous wind power (E_{wind}) is given by the following equation:

$$E_{wind} = \begin{cases} 0, & U < U_{min} \text{ or } U > U_{max} \\ 1/2\rho A U^3 & U_{min} \le U \le U_c \\ 1/2\rho A U_c^3 & U_c < U \le U_{max} \end{cases} \tag{3}$$

To convert the instantaneous wind speed (U) to daily mean wind speed ($\underline{U}$) which is available in CMIP6 model outputs, the wind speed is assumed to conform to a two-parameter Weibull distribution[9,41]:

$$p(U) = \frac{k}{\lambda}\left(\frac{U}{\lambda}\right)^{k-1} \exp\left[-\left(\frac{U}{\lambda}\right)^k\right] \tag{4}$$

where $p(U)$ represents the probability density function of instantaneous wind speed. The shape parameter k is chosen as 2, which falls within the recommended range given by ref. 41. The scale parameter λ in this equation is then derived from the known daily mean wind speed, $\underline{U}$:

$$\lambda = \frac{\underline{U}}{\Gamma\left(\frac{3}{2}\right)} \tag{5}$$

where $\Gamma()$ is the gamma function. Assuming the air density and the swept area of wind blades are both constants, we get the following out of equations (2) and (3):

$$\int E_{wind}(U)\,p(U)\,\mathrm{d}U \propto \lambda^3 \int_{\left(\frac{4}{\lambda}\right)^2}^{\left(\frac{13.5}{\lambda}\right)^2} u^{\frac{3}{2}} \mathrm{e}^{-u}\mathrm{d}u + 13.5^3\left[\mathrm{e}^{-\left(\frac{13.5}{\lambda}\right)^2} - \mathrm{e}^{-\left(\frac{25}{\lambda}\right)^2}\right] \tag{6}$$

where the left-hand side is the daily mean wind power production, suggesting that the daily wind power production is proportional to a function of λ. Combining it with equation (5), we can conclude that the daily wind power production is proportional to a function of daily mean wind speed ($\underline{U}$). Therefore, we will use the right-hand side of equation (6) substituting equation (5) for λ to estimate the relative size of daily wind power production afterwards.

We used the wind speed at 150 m height above the surface to represent the wind speed across the rotor plane. Wind speed at this height is approximated using the power law[9,42]:

$$\underline{U} = \underline{U_{10}}\left(\frac{150}{10}\right)^{\alpha} \tag{7}$$

Here, $\underline{U_{10}}$ is the daily mean wind speed at 10 m extracted from CMIP6 model outputs. The α is a coefficient often approximated as 1/7. Equation (7) will be substituted in equation (5) to compute.

Since we focus on relative changes of E_{wind} from the present climate to the future climate, other factors affecting the realistic E_{wind}, like the rotor diameter and swept area, are considered as constant and would not affect our results.

Solar power density

Solar power production mostly depends on solar irradiance but is also influenced by ambient temperature, wind speed and so on, on power output efficiency. Following previous efforts[4,10], we take solar radiance, ambient temperature and wind speed as input and simulate PV power generation per 1 m^2 of PV panel (E_{PV}):

$$E_{PV} = I \times \eta_{PV} \tag{8}$$

where I is the solar radiance on the PV module per m^2 (W m^{-2}) and η_{PV} is the efficiency of the PV module, which is influenced by weather conditions. Parameter η_{PV} can be computed as:

$$\eta_{PV} = \eta_{panel} \times (1 + \gamma \times (T_{panel} - T_{STC})) \tag{9}$$

where η_{panel} is the assumed panel efficiency under standard conditions (17%); γ is the typical efficacy response of monocrystalline silicon solar panels (−0.005 °C^{-1}); T_{STC} is the panel temperature under standard conditions (25 °C); and T_{panel} is the panel temperature corrected with temperature, irradiation and wind:

$$T_{panel} = c_1 + c_2 \times T + c_3 \times I + c_4 \times V \tag{10}$$

where c_1 is 4.3 °C; c_2 is 0.943; T is ambient temperature (°C); I is the solar radiance on the PV module (W m^{-2}); and c_4 is −1.528 °C s m^{-1} and V is the surface wind speed (m s^{-1}). Therefore, when T_{panel} surpass T_{STC}, the declined panel efficiency would further reduce E_{PV}.

Like wind power simulations, since we focus on climate impacts on E_{PV}, other factors affecting the realistic E_{PV}, such as the packing factor, are considered as constant and would not affect our results.

Climate change impact analysis procedures

The analysis procedures of climate change impact on energy supply, demand and SDM are listed step by step as follows:

Step 1: Choose a local energy planner or stakeholder at one grid cell.

Step 2: Assume the energy planner aims for a local energy system with dependence on wind or solar energy supply and the planned dependence can be achieved under present climate, denoted by $SDM_{present}$. $SDM_{present}$ is assumed to be 25%, 50% and 75% for low, medium and high levels of dependence scenarios, respectively.

Step 3: The energy planner determines the absolute number of baseline demand (D_{base}), which largely depends on the interested scale and stakeholder's socioeconomic factors and does not respond to temperature. Daily demand and total demand (D_{total}) can be derived according to the following equation (11). D_{total} refers to the sum of D_{base}, heating demand (D_{heat}) and cooling demand (D_{cool}). Please refer to the following section on Climate change impacts on supply and demand for details.

Step 4: Calculate the daily wind or solar power density ($E_{wind/PV}$) under present climate.

- For wind, refer to equations (2)–(7).
- For solar, refer to equations (8)–(10).

Step 5: Calculate the required IA of wind or solar plants to achieve the $SDM_{present}$ by solving the following equation (12). Note that, if required IC is not allowed due to realistic constraints, for example, policy or limited deployable areas, the planned $SDM_{present}$ is not suitable in this case.

Step 6: Calculate the supply and demand under future climate. To isolate climate change impacts, only climate impact-drivers (wind speed, temperature and radiation) are allowed to modulate supply, demand and resulting SDM, while non-climatic conditions (for example, system infrastructures) are kept constant.

- Relative changes of supply (%) are not influenced by IA but only caused by changes in wind/solar power density.
- Relative changes of demand (%) are not influenced by D_{base} but only caused by changes in temperature.

Step 7: Calculate SDM_{future} on the basis of future supply and demand according to equation (1). The change from $SDM_{present}$ to SDM_{future} is only influenced by climate-driven relative changes in supply and demand but is not influenced by D_{base} and IA. In addition, control experiments are performed to disentangle relative contributions of climate mean-induced supply/demand mean and climate variability-induced supply/demand variability to SDM changes. Please refer to the following section on Climate change impacts on supply–demand match for details.

Step 8: Implications for local energy planner or stakeholder. If SDM_{future} is lower than $SDM_{present}$, it would require additional supply to meet the demand in the context of planned level of dependence on wind/solar energy supply. Otherwise, the SDMM would cause power outages.

In addition, a relevant example can be found in Supplementary Note 1.

Climate change impacts on supply and demand

For the demand, we focus on relative changes of the temperature-responsive heating and cooling demand caused by climate change. The actual daily heating and cooling demand profile in a planned energy system is not available. However, many previous efforts robustly showed that intra-annual variations of heating and cooling demand always strongly depend on temperature[18–20,22,23]: hot days lead to higher demand for cooling and cold days lead to higher demand for heating. Therein, there are three most critical parameters: (1) the temperature that minimizes demand, i.e. the temperature corresponding to D_{base} (T_{base}); (2) the sensitivity of demand changes to heating (β_{heat}): the percentage increment of demand relative to D_{base} per 1 °C when $T < T_{base}$; and (3) the sensitivity of demand changes to cooling (β_{cool}): the percentage increment of demand relative to D_{base} per 1 °C when $T > T_{base}$. We compiled previous literature and found that T_{base}, β_{heat} and β_{cool} are not uniform, varying with many local conditions (infrastructure, social-economic conditions, custom and so on). They probably lie in a range as below: T_{base} spans from 12 to 22 °C; β_{heat} spans from 2% to 5% per °C; and β_{cool} spans from 3% to 8% per °C. Since these parameters are not available at every location at the global scale, we propose two scenarios at each location that can mostly capture the range of demand responses to temperature: (1) a high-sensitivity one: T_{base} = 18 °C, β_{cool} = 5% per °C and β_{heat} = 8% per °C; and (2) a low-sensitivity one: T_{base} = 18 °C, β_{heat} = 2% per °C and β_{cool} = 3% per °C.

The absolute number of D_{base} in this study is decided by any energy system planner or stakeholder within one grid cell (around 110 × 110 km^2 at the equator). The local energy system may be a few households, a county or a city. Given D_{base}, T_{base}, β_{heat}, β_{cool} and present T_t (T at day t), the present daily demand profiles and $D_{total,\,present}$ can be derived by solving equation (11).

$$\begin{aligned} D_{total} &= \sum_{1}^{n}(D_{cool,t} + D_{heat,t} + D_{base}),\ t \in [1,n] \\ D_{cool,t} &= \begin{cases} (T_t - T_{base}) \times \beta_{cool} \times D_{base}, & T_t \geq T_{base} \\ 0, & T_t < T_{base} \end{cases} \\ D_{heat,t} &= \begin{cases} (T_{base} - T_t) \times \beta_{heat} \times D_{base}, & T_t \leq T_{base} \\ 0, & T_t > T_{base} \end{cases} \end{aligned} \tag{11}$$

With climate change, we apply future T, constant D_{base}, β_{heat}, β_{cool} and equation (11) to derive future daily demand profiles and future total demand. Therefore, climate change impacts on demand are only due to changes in T. We acknowledge potential nonlinearity of the heating

and cooling demand response in the tails of temperature distribution but do not account for them due to the lack of data.

For the supply, daily variations of supply are computed on the basis of the wind and solar power density and the IA. We applied the climate simulations from 12 GCMs to compute the global wind and solar power density productions under present climate (1985–2014) and future climate. Given each $SDM_{present}$, present daily demand and present daily power density, the required IA of wind or solar plants can be derived according to equation (12).

$$S_t = IA_{wind/PV} \times E_{wind/PV,t}, t \in [1, n]$$
$$D_{met,t} = \begin{cases} D_t, S_t \geq D_t \\ S_t, S_t < D_t \end{cases} \quad (12)$$
$$SDM_{present} = \frac{\sum_1^n D_{met,t}}{\sum_1^n D_t} \times 100\%$$

where t is time step under present climate; S is present wind or solar supply (kWh d^{-1}); IA is installation area (m^2); E is present power density (kWh d^{-1} m^2); D is present demand (kWh d^{-1}); and D_{met} is demand met by supply (kWh d^{-1}). Then, supply profiles under present climate ($S_{present}$) are derived by scaling present power density profiles with IA. With climate change, we apply simulated future power density profiles and constant IA to determine future supply profiles (S_{future}) as well. Therefore, the climate impact on supply here is only caused by changes in climate-driven power density (E).

Climate change impacts on supply–demand match

The SDM is quantified by the fraction of total demand met by wind or solar supply over a temporal period, as equation (1): 100% means a full match; 0% means a least match. For each grid cell, we ensure the same $SDM_{present}$ under present climate (1985–2014). The climate change impacts on SDM can be derived by taking the percentage differences between the two periods ($\Delta SDM = (SDM_{future} - SDM_{present})/SDM_{present} - 100\%$).

First, we assess climate change impacts on the supply and demand separately and try to disentangle their respective consequences on SDM. To investigate SDM changes driven by the supply alone, we use present and future supply profiles (daily time series) but control demand is invariant to temperature changes (that is, demand is constant over time). Hence, present and future profiles only differ in the supply and it allows the isolation of climate change impacts on SDM caused by the supply alone. We also directly replace future demand profiles with present demand profiles (that is, demand is not constant but can vary with daily temperature), the resulting changes in SDM are similar (Supplementary Fig. 11). To investigate the SDM changes driven by the demand alone, we use present and future demand profiles but replace future supply profiles with present supply profiles. Hence, present and future profiles only differ in the demand and it allows the isolation of climate change impacts on SDM caused by the demand alone.

Second, we combine present and future supply and demand together and explore whether combining them would 'counterbalance' or 'enlarge' SDM changes driven by supply/demand alone. In this case, present and future supply and demand profiles are all used. Hence, the differences in SDM are caused by the synthesized effects of supply and demand.

Third, since climate change includes both changes in climate mean (long-term mean of climate state) and climate variability (day-to-day variability), we also perform control experiments to disentangle their relative contributions to SDM changes. To isolate the part of climate variability, for instance, we control $\mu_{S_{present}} = \mu_{S_{future}}$ by weighting future profiles with a ratio: $S_{future} = S_{future}\mu_{S_{present}}/\mu_{S_{future}}$. μ is the mean temporal value for each grid cell. Hence, present and 'adjusted' future supply profiles only differ in the variability and it allows the isolation of climate change impacts on supply-induced SDM caused by the climate variability alone. To isolate the part of climate mean, future supply profiles are equal to present profiles in variability by replacing future profiles with weighted present profiles: $S_{future} = S_{present}\mu_{S_{future}}/\mu_{S_{present}}$. Hence, present and 'adjusted' future profiles only differ in the mean and it allows the isolation of climate change impacts caused by the climate mean alone. We apply the same attribution approach to demand profiles or supply–demand profiles together. The verification suggests that the attribution approach is reliable (Supplementary Fig. 12).

In addition, by adopting the general framework from climate science to investigate climate and weather extremes (for example, droughts and heatwaves), we define daily SDMM (100% − SDM) and two finer metrics: (1) SDMM frequency: the proportion of days with daily SDM < 100% and (2) SDMM intensity: the average fraction of unmet demand to total demand during days with daily SDM < 100%. These two metrics provide finer characteristics of daily SDMM changes from climate change.

Climate change adaptation

To adapt to climate change negative impacts on SDM, two strategies are proposed:

(1) Adding IA into the future energy system: we add IA_{wind} and IA_{PV} by 1–100% in the future. Therefore, the future wind and solar supply is anticipated to increase and match more demand. Comparing new SDM_{future} at different IA levels with $SDM_{present}$ can determine whether new SDM_{future} can recover to $SDM_{present}$. If yes, we can derive the precise level of IA needed.

(2) Adding energy storage into the future energy system: we add energy storage with the size ranging from 1 to 20 days in the future. For instance, 1 day means the storage can store 1 unit of averaged daily demand under present climate. If the supply could meet the demand, storage would be charged with excess supply, if available, until the storage is full, after which supply can be curtailed. By contrast, if supply cannot meet demand, storage, if available, would be discharged to fill the demand gap until storage is emptied. Therefore, the supply is better used to match demand, which is likely to increase SDM. Comparing new SDM_{future} at different energy storage sizes with $SDM_{present}$ can determine whether new SDM_{future} can recover to $SDM_{present}$. If yes, we can derive the precise energy storage size needed.

Midterm climate change impacts

To investigate midterm climate change impacts on SDM of global wind and solar energy systems, we calculate the differences of SDM between future midterm climate (2041–2070) and present climate (1985–2014); that is, $\Delta SDM = (SDM_{2041-2070} - SDM_{1985-2014})/SDM_{1985-2014} \times 100\%$. As expected, compared to long-term impacts, Supplementary Fig. 13 shows that midterm climate change impacts on SDM are much smaller in magnitude (lowered by 42% and 49% for wind and solar systems on average). These results suggest that climate change impacts on SDM of wind and solar energy systems depend on the global warming level, timing and so on.

All estimates are first computed separately for each of the CMIP6 GCMs and are then regridded to the horizontal resolution of 1° × 1° for further analyses. Stippling in the plots indicates regions where the detected changes are robust; that is, 9 out of 12 models in the cluster agree on the sign of the changes.

Data availability

Climate model simulations are publicly available from Earth System Grid Federation: https://esgf-node.llnl.gov/search/cmip6/. Source data are provided with this paper.

Code availability

Codes are publicly available at Zenodo: https://doi.org/10.5281/zenodo.6884124.

References

1. *World Energy Outlook* (International Energy Agency, 2021).
2. Davis, S. J. et al. Net-zero emissions energy systems. *Science* **360**, eaas9793 (2018).
3. He, G. et al. Rapid cost decrease of renewables and storage accelerates the decarbonization of China's power system. *Nat. Commun.* **11**, 2486 (2020).
4. Gernaat, D. E. H. J. et al. Climate change impacts on renewable energy supply. *Nat. Clim. Change* **11**, 362 (2021).
5. van Ruijven, B. J., De Cian, E. & Wing, I. S. Amplification of future energy demand growth due to climate change. *Nat. Commun.* **10**, 2762 (2019).
6. Arvizu, D. et al. in *IPCC Special Report on Renewable Energy Sources and Climate Change Mitigation* (eds Edenhofer, O. et al.) (Cambridge Univ. Press, 2011).
7. Clark, L. et al. in *Climate Change 2022: Mitigation of Climate Change* (eds Shukla, P. R. et al.) 666–670 (Cambridge Univ. Press, 2022).
8. Yalew, S. G. et al. Impacts of climate change on energy systems in global and regional scenarios. *Nat. Energy* **5**, 794–802 (2020).
9. Pryor, S. C., Barthelmie, R. J., Bukovsky, M. S., Leung, L. R. & Sakaguchi, K. Climate change impacts on wind power generation. *Nat. Rev. Earth Environ.* **1**, 627–643 (2020).
10. Feron, S., Cordero, R. R., Damiani, A. & Jackson, R. B. Climate change extremes and photovoltaic power output. *Nat. Sustain.* **4**, 270–276 (2021).
11. Pryor, S. C. & Barthelmie, R. J. A global assessment of extreme wind speeds for wind energy applications. *Nat. Energy* **6**, 268–276 (2021).
12. Wohland, J. Process-based climate change assessment for European winds using EURO-CORDEX and global models. *Environ. Res. Lett.* **17**, 124047 (2022).
13. Allen, M. R., Fernandez, S. J., Fu, J. S. & Olama, M. M. Impacts of climate change on sub-regional electricity demand and distribution in the southern United States. *Nat. Energy* **1**, 16103 (2016).
14. Mays, J. et al. Private risk and social resilience in liberalized electricity markets. *Joule* **6**, 369–380 (2022).
15. Bruch, M. et al. *Power Blackout Risks: Risk Management Options Emerging Risk Initiative* (CRO Forum, 2011).
16. Karnauskas, K. B., Lundquist, J. K. & Zhang, L. Southward shift of the global wind energy resource under high carbon dioxide emissions. *Nat. Geosci.* **11**, 38–43 (2018).
17. Cong, S. C., Nock, D., Qiu, Y. L. & Xing, B. Unveiling hidden energy poverty using the energy equity gap. *Nat. Commun.* **13**, 2456 (2022).
18. Wenz, L., Levermann, A. & Auffhammer, M. North–south polarization of European electricity consumption under future warming. *Proc. Natl Acad. Sci. USA* **114**, E7910–E7918 (2017).
19. Auffhammer, M., Baylis, P. & Hausman, C. H. Climate change is projected to have severe impacts on the frequency and intensity of peak electricity demand across the United States. *Proc. Natl Acad. Sci. USA* **114**, 1886–1891 (2017).
20. Isaac, M. & van Vuuren, D. P. Modeling global residential sector energy demand for heating and air conditioning in the context of climate change. *Energy Policy* **37**, 507–521 (2009).
21. Rode, A. et al. Estimating a social cost of carbon for global energy consumption. *Nature* **598**, 308–314 (2021).
22. Deroubaix, A. et al. Large uncertainties in trends of energy demand for heating and cooling under climate change. *Nat. Commun.* **12**, 5197 (2021).
23. De Cian, E. & Wing, I. S. Global energy consumption in a warming climate. *Environ. Resour. Econ.* **72**, 365–410 (2019).
24. Jerez, S. et al. The impact of climate change on photovoltaic power generation in Europe. *Nat. Commun.* **6**, 10014 (2015).
25. Seneviratne, S. I. et al. in *Climate Change 2021: The Physical Science Basis* (eds Masson-Delmotte, V. et al.) 1513–1766 (Cambridge Univ. Press, 2021).
26. Mastrucci, A., van Ruijven, B., Byers, E., Poblete-Cazenave, M. & Pachauri, S. Global scenarios of residential heating and cooling energy demand and CO_2 emissions. *Clim. Change* **168**, 14 (2021).
27. Zeyen, E., Hagenmeyer, V. & Brown, T. Mitigating heat demand peaks in buildings in a highly renewable European energy system. *Energy* **231**, 120784 (2021).
28. Bell, N. O., Bilbao, J. I., Kay, M. & Sproul, A. B. Future climate scenarios and their impact on heating, ventilation and air-conditioning system design and performance for commercial buildings for 2050. *Renew. Sust. Energy Rev.* **162**, 112363 (2022).
29. Liu, L. et al. Optimizing wind/solar combinations at finer scales to mitigate renewable energy variability in China. *Renew. Sustain. Energy Rev.* **132**, 110151 (2020).
30. Shaner, M. R., Davis, S. J., Lewis, N. S. & Caldeira, K. Geophysical constraints on the reliability of solar and wind power in the United States. *Energy Environ. Sci.* **11**, 997–997 (2018).
31. Perera, A. T. D., Nik, V. M., Chen, D. L., Scartezzini, J. L. & Hong, T. Z. Quantifying the impacts of climate change and extreme climate events on energy systems. *Nat. Energy* **5**, 150–159 (2020).
32. Bartos, M. et al. Impacts of rising air temperatures on electric transmission ampacity and peak electricity load in the United States. *Environ. Res. Lett.* **11**, 114008 (2016).
33. Liu, L. B. et al. Potential contributions of wind and solar power to China's carbon neutrality. *Resour. Conserv. Recycl.* **180**, 106155 (2022).
34. Kittner, N., Lill, F. & Kammen, D. M. Energy storage deployment and innovation for the clean energy transition. *Nat. Energy* **2**, 17125 (2017).
35. Winterfeldt, J. & Weisse, R. Assessment of value added for surface marine wind speed obtained from two regional climate models. *Mon. Weather Rev.* **137**, 2955–2965 (2009).
36. Carvalho, D., Rocha, A., Costoya, X., DeCastro, M. & Gomez-Gesteira, M. Wind energy resource over Europe under CMIP6 future climate projections: what changes from CMIP5 to CMIP6. *Renew. Sust. Energy Rev.* **151**, 111594 (2021).
37. Kozarcanin, S., Liu, H. L. & Andresen, G. B. 21st century climate change impacts on key properties of a large-scale renewable-based electricity system. *Joule* **3**, 992–1005 (2019).
38. Craig, M. T., Carreno, I. L., Rossol, M., Hodge, B. M. & Brancucci, C. Effects on power system operations of potential changes in wind and solar generation potential under climate change. *Environ. Res. Lett.* **14**, 034014 (2019).
39. Craig, M. T. et al. Overcoming the disconnect between energy system and climate modeling. *Joule* **6**, 1405–1417 (2022).
40. IPCC: Summary for Policymakers. In *Climate Change 2021: The Physical Science Basis* (eds Masson-Delmotte, V. et al.) (Cambridge Univ. Press, 2021).
41. Pryor, S. C., Nielsen, M., Barthelmie, R. J. & Mann, J. Can satellite sampling of offshore wind speeds realistically represent wind speed distributions? Part II: Quantifying uncertainties associated with distribution fitting methods. *J. Appl. Meteorol.* **43**, 739–750 (2004).
42. Irwin, J. S. Theoretical variation of the wind profile power-law exponent as a function of surface-roughness and stability. *Atmos. Environ.* **13**, 191–194 (1979).

43. Iturbide, M. et al. An update of IPCC climate reference regions for subcontinental analysis of climate model data: definition and aggregated datasets. *Earth Syst. Sci. Data* **12**, 2959–2970 (2020).

Acknowledgements

We acknowledge the World Climate Research Programme, which, through its Working Group on Coupled Modelling, coordinated and promoted CMIP6. We thank the climate modelling groups for producing and making available their model output, the Earth System Grid Federation (ESGF) for archiving the data and providing access and the multiple funding agencies who support CMIP6 and ESGF. We thank all contributors to the CMIP6 experiments. We thank W. Jan for useful discussions. We thank B. Zhu for producing material images used in Fig. 1. This study is funded by the Second Tibetan Plateau Scientific Expedition and Research Program (no. 2019QZKK1001) and National Natural Science Foundation of China (no. 42230506). L.L. acknowledges support from China Scholarship Council (no. 201806010309); G.H. acknowledges support from the Global Energy Initiative at ClimateWorks Foundation (no. 23-2515); and G.L. acknowledges support from the National Natural Science Foundation of China (no. 71991484).

Author contributions

L.L. conceived the original idea. L.L. and M.W. designed the experiments with contributions from G.H. S.L. and M.W. conducted the wind energy assessments. L.L. conducted all other data analyses. L.L. drafted the paper with contributions from all co-authors.

Competing interests

The authors declare no competing interests.

Additional information

Supplementary information The online version contains supplementary material available at https://doi.org/10.1038/s41560-023-01304-w.

Correspondence and requests for materials should be addressed to Laibao Liu or Mengxi Wu.

Peer review information *Nature Energy* thanks Bastiaan van Ruijven and the other, anonymous, reviewer(s) for their contribution to the peer review of this work.